RSC Advances

COMMUNICATION

View Article Online
View Journal | View Issue

Fe^{3+} facilitating the response of NiO towards H_2S†

Fang Li, Yuejiao Chen and Jianmin Ma*

Cite this: *RSC Adv.*, 2014, **4**, 14201

Received 8th January 2014
Accepted 27th February 2014

DOI: 10.1039/c4ra00182f

www.rsc.org/advances

Fe_2O_3-loaded NiO nanoplates have been successfully prepared by a facile method by immersing NiO nanoplates in aqueous $Fe(NO_3)_3$ solution and annealing the corresponding as-immersed NiO nanoplates. When studied as sensing materials, the as-fabricated Fe_2O_3-loaded NiO nanoplates display enhanced response towards H_2S in comparison with pure NiO nanoplates.

Gas sensing has been widely studied owing to its important applications in environmental monitoring. Gas-sensing performance usually depends on the as-employed sensing materials. So far, many semiconductors have been explored as important sensing materials, such as Fe_2O_3,[1,2] ZnO,[3,4] WO_3,[5,6] SnO_2,[7,8] CuO,[9,10] TiO_2,[11,12] NiO[13,14] and Co_3O_4,[15,16] *etc.* Moreover, other strategies have also been employed to improve the sensing performance, such as noble metal doping oxides,[17–19] heterogeneous oxides,[20–22] and carbon or polymer/oxides,[23–26] *etc.*

As one of most important p-type sensing semiconductors, various NiO materials have been studied.[13,14,27–30] However, pure NiO usually has relatively poor sensing properties. Much effort has been made to modify NiO nanostructures to achieve excellent gas-sensing properties.[31–35] For example, NiO@ZnO heterostructured nanotubes fabricated by the coelectrospinning method improved H_2S-sensing properties owing to the change of nanostructure and activity of ZnO and NiO nanocrystals as well as combination of homo- and heterointerfaces.[31] Nguyen *et al.* reported that the response of the NiO-decorated SnO_2 nanowire sensor to 10 ppm H_2S at 300 °C reached as high as 1372 owing to the catalytic effect of NiO and the formation of a continuous chain of n–p–n–p junctions.[32] Inspired by these examples, exploring an alternative, facile decorating method is highly desirable.

Fe_2O_3 is a well-known H_2S-sensing material.[1,2,36–38] Thus, it is expected that loading Fe_2O_3 on NiO nanoplates could exhibit high response towards H_2S gas. In this communication, we have prepared the Fe_2O_3-loaded NiO nanoplates through immersing hydrothermally proceeded NiO nanoplates with aqueous $Fe(NO_3)_3$ solution and annealing the corresponding as-immersed NiO nanoplates. The as-fabricated Fe_2O_3-loaded NiO nanoplates have largely enhanced the response towards H_2S in comparison with pure NiO nanoplates.

The Fe_2O_3-loaded NiO nanoplates were prepared by two steps: (1) NiO nanoplates were obtained through annealing hydrothermally proceeded $Ni(OH)_2$ nanoplates with the assistance of *n*-butylamine;[38] (2) Fe_2O_3-loaded NiO nanoplates were produced through annealing immersed NiO nanoplates with aqueous $Fe(NO_3)_3$ solution. The phase of NiO and Fe_2O_3-loaded NiO was analyzed by X-ray diffraction (XRD). In Fig. 1, one could find that all the peaks in patterns could be attributed to these of the standard card (PDF: 47-1049).[39] There is no diffraction peak of Fe_2O_3 observed for the XRD pattern of Fe_2O_3-loaded NiO

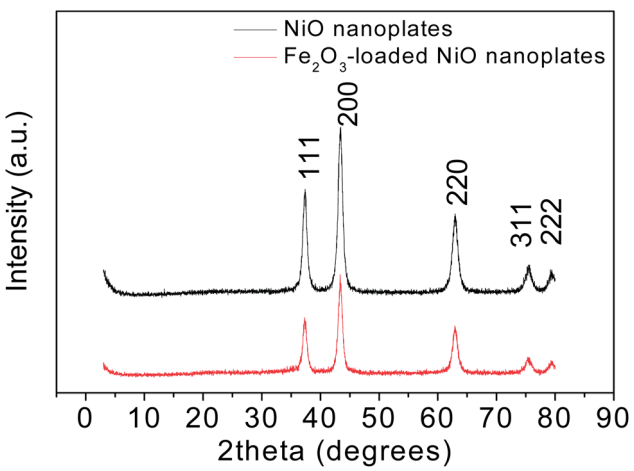

Fig. 1 XRD pattern for NiO nanoplates and Fe_2O_3-loaded NiO nanoplates.

Key Laboratory for Micro-Nano Optoelectronic Devices of Ministry of Education, State Key Laboratory for Chemo/Biosensing and Chemometrics, Hunan University, Changsha, P. R. China. E-mail: nanoelechem@hnu.edu.cn

† Electronic supplementary information (ESI) available. See DOI: 10.1039/c4ra00182f

nanoplates, which indicate that the content of Fe_2O_3 is extremely low. The content of Fe_2O_3-loaded NiO nanocomponents is about 3.9% by weight, as supported by EDX (Fig. S1†).

The morphology, composition and elemental distribution of the as-fabricated Fe_2O_3-loaded NiO nanoplates were further mapped through TEM and EDS by displaying the integrated intensity of oxygen, nickel and iron signals as a function of the beam position when operating the TEM in scanning mode (STEM). The SEM image of NiO without Fe_2O_3 loading (Fig. 2a) shows the hexagonal nanoplates, similar to our previous report.[39] The as-fabricated Fe_2O_3-loaded NiO sample (Fig. 2b) is composed of hexagonal nanoplates, which is similar to the unloaded NiO nanoplates. Fig. 2c shows an HAADF-STEM image of the Fe_2O_3-loaded NiO nanoplate. The results shown in Fig. 2d–f reveal that the three elements of O, Ni, and Fe are distributed very homogeneously in the nanoplate. Moreover, the Fe/Ni ratio measured from the nanoplates with EDS analysis show an average ratio of 72.03 : 2.63. The mapping data indicates that our as-employed method is effective for us to prepare Fe_2O_3-loaded NiO nanoplates.

To understand the gas-sensing properties of Fe_2O_3-loaded NiO nanoplates, we compared the response characteristics of NiO nanoplates and Fe_2O_3-loaded NiO nanoplates-based gas sensor, respectively. Fig. 3a and b display that the typical response and recovery time of two sensors to 10 ppm H_2S at different temperature. From Fig. 3a, it could be found that the response of the two sensors have the same change trend, the response increases with the increase of operating temperature at the beginning, and approaches a maximum value at 200 °C (named as the optimum operating temperature), however, gradually decreases with further increasing operating temperature. The response of Fe_2O_3-loaded NiO nanoplates is constantly higher than that of NiO nanoplates at different temperatures. Moreover, the recovery time of NiO nanoplates and Fe_2O_3-loaded NiO nanoplates were also studied, as shown in Fig. 3b. The recovery time vary from 27 to 13 s (from 25 to 350 °C) for Fe_2O_3-loaded NiO nanoplates, which did not change much when changing the operating temperature. However, the recovery time of NiO nanoplates dropped dramatically with the temperature increasing from 25 to 250 °C. Analyzed from the data of their response and recovery time, we chose 200 °C as the working temperature.

To understand the sensing characteristics of two sensors, the real-time response curves of Fe_2O_3-loaded NiO sensor and NiO sensor to H_2S gas with increased concentration ranging from 1 to 100 ppm at a working temperature of 200 °C were investigated, as shown in Fig. 4a and b, respectively. In Fig. 4a and b, one could find that gas responses increase with the increase of H_2S concentration. As shown in Fig. 4c, the Fe_2O_3-loaded NiO nanoplate sensor shows the response of approximately 2.89, 3.8, 7.35, 13.8, 26.48, and 109.4 for the corresponding 1, 5, 10, 20, 50, and 100 ppm H_2S gas, respectively. In comparison, the NiO nanoplates based sensor shows response of approximately 1.64, 1.82, 2.94, 3.95, 3.83, and 10.19 for the corresponding 1, 5, 10, 20, 50,

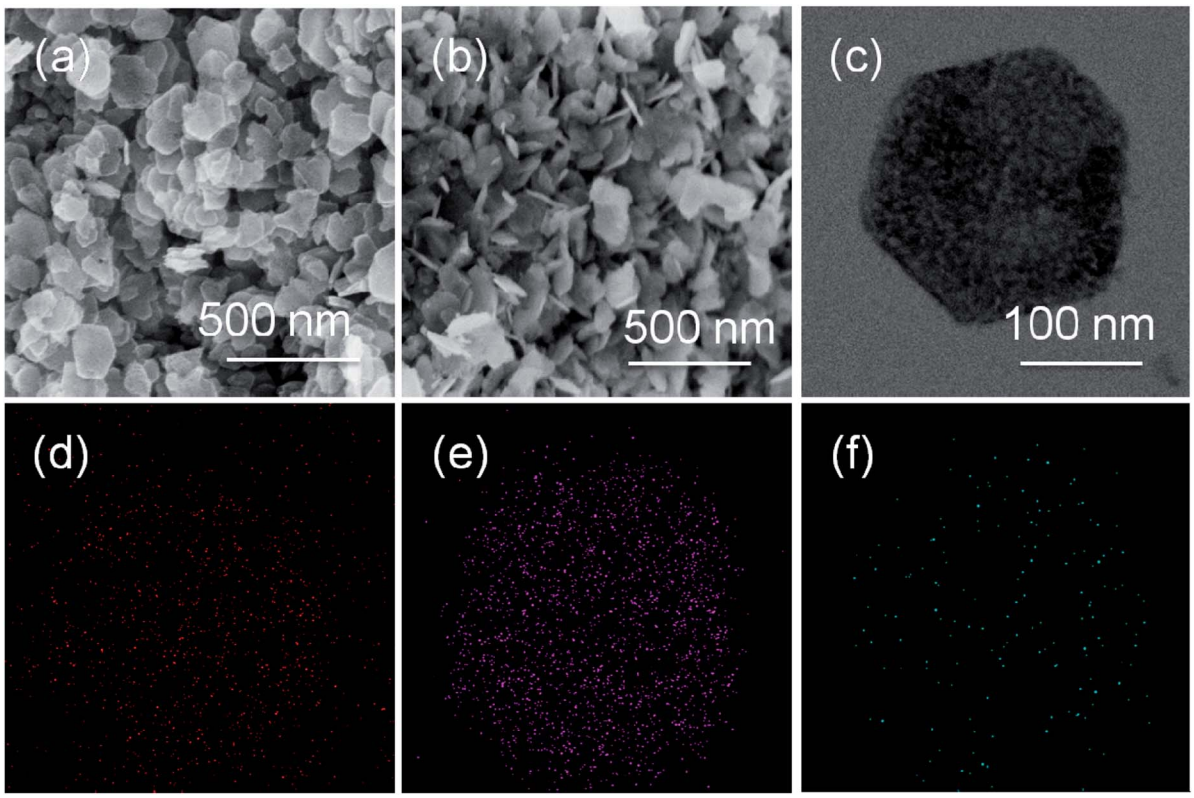

Fig. 2 (a and b) SEM images of NiO nanoplates and Fe_2O_3-loaded NiO nanoplates, respectively; STEM-EDS elemental maps of as-fabricated Fe_2O_3-loaded NiO nanoplates: (c) HAADF-STEM image, (d) O elemental map, (e) Ni elemental map, and (f) Fe elemental map.

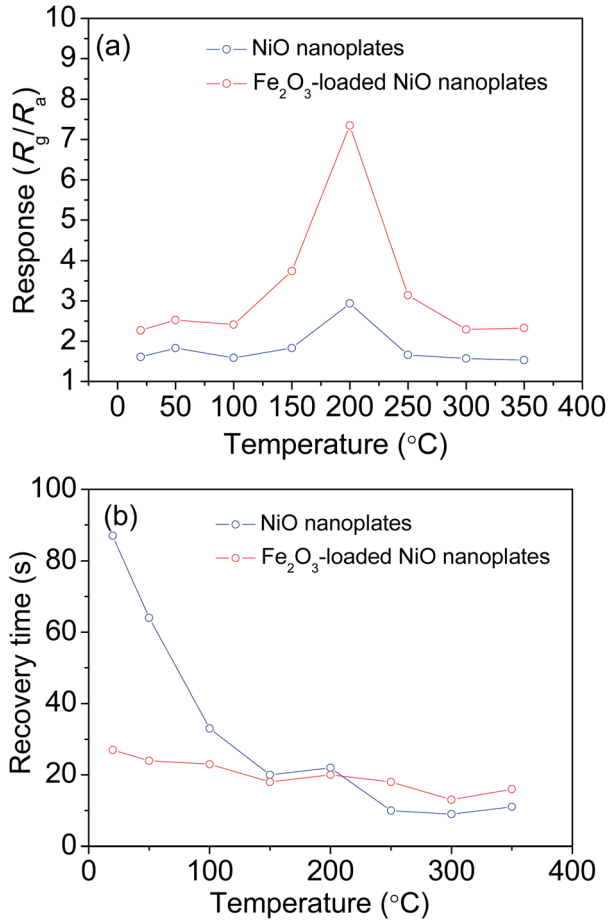

Fig. 3 (a) Response and (b) recovery time of NiO nanoplate and Fe_2O_3-loaded NiO nanoplate sensors to 10 ppm H_2S gas at different working temperature.

and 100 ppm H_2S gas, respectively. It is clearly found that the response of NiO nanoplates towards H_2S gas after loading Fe_2O_3 is improved dramatically. The response is compared with those results reported by some literatures.[1,2] However, the sensing mechanism of NiO and Fe_2O_3-loaded NiO sensor towards H_2S gas is different from those reported literatures involved Fe_2O_3.[1,2] The gas-sensing behavior of the p-type NiO semiconductor towards H_2S gas can be explained by the decrease in the hole concentration due to the increased formation of negatively charged oxygen upon exposure to the oxidizing gas (H_2S). After injection of H_2S gas, H_2S molecules were adsorbed on the surface, providing electrons to the surface of NiO nanoplates. During this process the potential barrier increased and hence the resistance of the oxide was enhanced. Moreover, owing to extrahigh molar ratio of NiO to Fe_2O_3, the Fe_2O_3-loaded NiO nanoplates show the gas-sensing behavior of p-type semiconductors towards H_2S gas. The NO_2-sensing performance of Fe_2O_3-loaded NiO nanoplates are largely improved owing to the change of nanostructure and activity of NiO and Fe_2O_3 as well as combination of homo- and heterointerfaces.[31]

To further confirm the versatility of as-fabricated Fe_2O_3-loaded NiO nanoplate sensors, the selective test towards to 50 ppm CO, CH_4, SO_2 and H_2S was conducted at 200 °C, respectively.

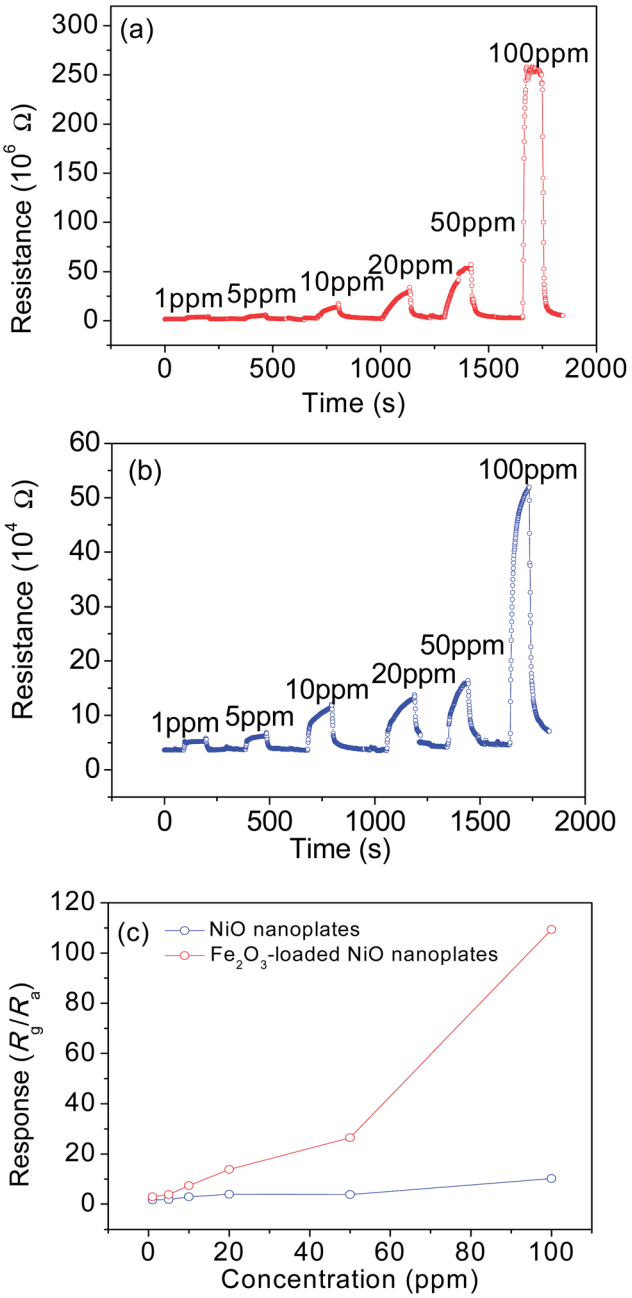

Fig. 4 (a and b) The real-time response curve of the Fe_2O_3-loaded NiO nanoplate and NiO nanoplate sensors to H_2S gas with increased concentration at a working temperature of 200 °C, respectively; (c) the relationship between the response and H_2S concentration.

Fig. 5 indicates that both of NiO nanoplate and Fe_2O_3-loaded NiO nanoplate sensors show excellent selectivity to H_2S gas. This indicates that the Fe_2O_3-loaded NiO nanoplate sensor has a quite wonderful selectivity to H_2S gas.

In Fig. 6a and b, the reproducibility and stability of the NiO nanoplate and Fe_2O_3-loaded NiO nanoplate sensors were also investigated. The results indicate that the Fe_2O_3-loaded NiO nanoplate sensor maintains 82.7% of its initial response amplitude after ten successive sensing tests to 50 ppm H_2S gas at 200 °C, which is better than that the NiO nanoplates (74.4%).

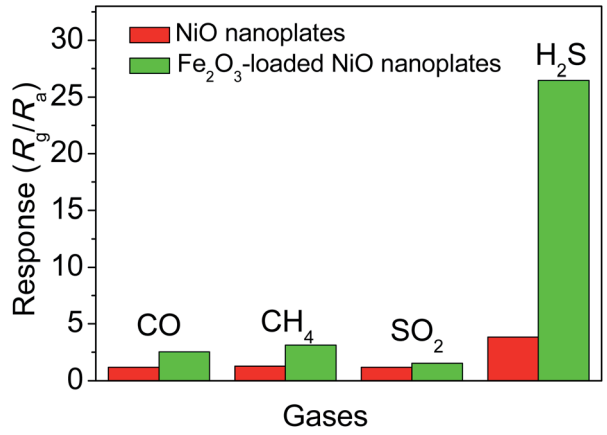

Fig. 5 Sensor response to various gases with 50 ppm at 200 °C.

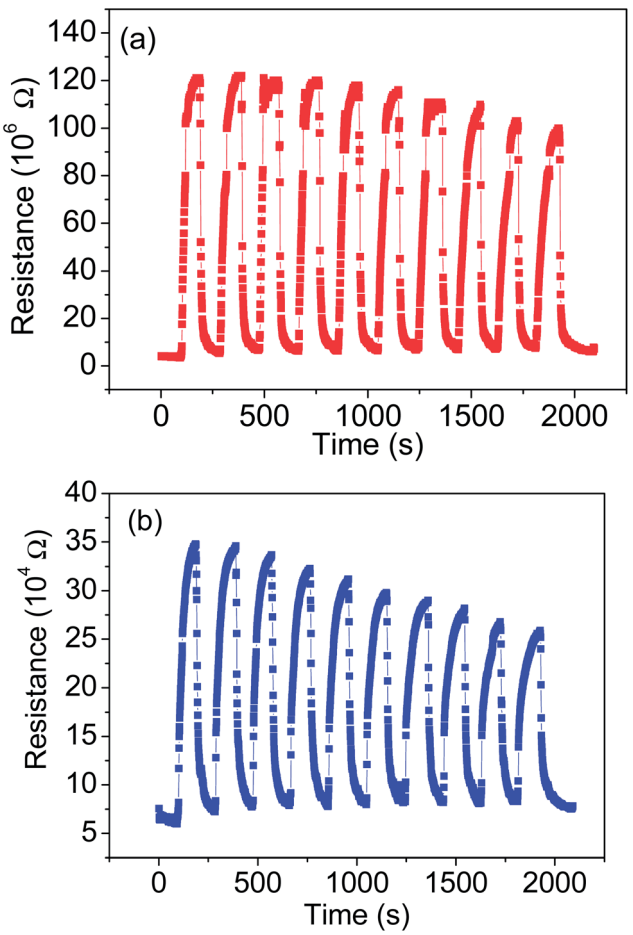

Fig. 6 (a and b) The reproducibility and stability of the Fe_2O_3-loaded NiO nanoplates and NiO nanoplates sensors to 50 ppm H_2S gas at 200 °C.

These results demonstrate that the Fe_2O_3-loaded NiO nanoplate sensor has better reproducibility and stability to H_2S gas than the NiO nanoplates sensor.

In summary, we have developed a synthetic route to prepare Fe_2O_3-loaded NiO nanoplates with high response, excellent selectivity towards H_2S gas. Our as-employed method to immerse NiO nanoplates with aqueous $Fe(NO_3)_3$ solution and anneal the corresponding as-immersed NiO nanoplates is proven to be effective to synthesize Fe_2O_3-loaded NiO nanoplates. The as-fabricated Fe_2O_3-loaded NiO nanoplates are promising H_2S-sensing materials due to its response as high as 26.48 and excellent selectivity towards 50 ppm H_2S gas.

Acknowledgements

This work was supported by the National Natural Science Foundation of China (Grant no. 51302079) and the Young Teachers' Growth Plan of Hunan University (Grant no. 2012-118).

Notes and references

1 J. M. Ma, L. Mei, Y. J. Chen, Q. H. Li, T. H. Wang, X. C. Duan and W. J. Zheng, *Nanoscale*, 2013, **5**, 895–898.
2 J. W. Deng, J. M. Ma, L. Mei, Y. J. Tang, Y. J. Chen, T. Lv, Z. Xu and T. H. Wang, *J. Mater. Chem. A*, 2013, **1**, 12400–12403.
3 S. Q. Tian, F. Yang, D. W. Zeng and C. S. Xie, *J. Phys. Chem. C*, 2012, **116**, 10586–10591.
4 J. Zhang, S. R. Wang, M. J. Xu, Y. Wang, B. L. Zhu, S. M. Zhang, W. P. Huang and S. H. Wu, *Cryst. Growth Des.*, 2009, **9**, 3532–3537.
5 J. M. Ma, J. Zhang, S. R. Wang, T. H. Wang, J. B. Lian, X. C. Duan and W. J. Zheng, *J. Phys. Chem. C*, 2011, **115**, 18157–18163.
6 D. L. Chen, X. X. Hou, H. J. Wen, Y. Wang, H. L. Wang, X. J. Li, R. Zhang, H. X. Lu, H. L. Xu, S. K. Guan, J. Sun and L. Gao, *Nanotechnology*, 2010, **21**, 035501.
7 J. M. Ma, J. Zhang, S. R. Wang, Q. H. Wang, L. F. Jiao, J. Q. Yang, X. C. Duan, Z. F. Liu, J. B. Lian and W. J. Zheng, *CrystEngComm*, 2011, **13**, 6077–6081.
8 R. Li, J. M. Du, Y. X. Luan, H. Zou, G. S. Zhuang and Z. H. Li, *CrystEngComm*, 2012, **14**, 3404–3410.
9 F. Zhang, A. W. Zhu, Y. P. Luo, Y. Tian, J. H. Yang and Y. Qin, *J. Phys. Chem. C*, 2010, **114**, 19214–19219.
10 D. P. Singh, A. K. Ojha and O. N. Srivastava, *J. Phys. Chem. C*, 2009, **113**, 3409–3418.
11 C. X. Wang, L. W. Yin, L. Y. Zhang, Y. X. Qi, N. Lun and N. N. Liu, *Langmuir*, 2010, **26**, 12841–12848.
12 M. H. Seo, M. Yuasa, T. Kida, J. S. Huh, K. Shimanoe and N. Yamazoe, *Sens. Actuators, B*, 2009, **137**, 513–520.
13 B. Liu, H. Q. Yang, H. Zhao, L. J. An, L. H. Zhang, R. Y. Shi, L. Wang, L. Bao and Y. Chen, *Sens. Actuators, B*, 2011, **156**, 251–262.
14 N. G. Cho, I. S. Hwang, H. G. Kim, J. H. Lee and I. D. Kim, *Sens. Actuators, B*, 2011, **156**, 366–371.
15 C. C. Li, X. M. Yin, T. H. Wang and H. C. Zeng, *Chem. Mater.*, 2009, **21**, 4984–4992.
16 C. W. Sun, S. Rajasekhara, Y. J. Chen and J. B. Goodenough, *Chem. Commun.*, 2011, **47**, 12852–12854.
17 X. Y. Xue, Z. H. Chen, C. H. Ma, L. L. Xing, Y. J. Chen, Y. G. Wang and T. H. Wang, *J. Phys. Chem. C*, 2010, **114**, 3968–3972.
18 X. H. Liu, J. Zhang, L. W. Wang, T. L. Yang, X. Z. Guo, S. H. Wu and S. R. Wang, *J. Mater. Chem.*, 2011, **21**, 349–356.

19 H. Kim, C. Jin, S. Park, S. Kim and C. Lee, *Sens. Actuators, B*, 2012, **161**, 594–599.
20 M. R. Yu, R. J. Wu and M. Chavali, *Sens. Actuators, B*, 2011, **153**, 321–328.
21 J. Kim, W. Kim and K. Yong, *J. Phys. Chem. C*, 2012, **116**, 15682–15691.
22 E. D. Gaspera, M. Guglielmi, S. Agnoli, G. Granozzi, M. L. Post, V. Bello, G. Mattei and A. Martucci, *Chem. Mater.*, 2010, **22**, 3407–3417.
23 G. Singh, A. Choudhary, D. Haranath, A. G. Joshi, N. Singh, S. Singh and R. Pasrich, *Carbon*, 2012, **50**, 385–394.
24 C. H. Zhan, Y. Z. Pan, Z. Wang, Y. F. Wang, H. F. He and Z. Y. Hou, *Sens. Actuators, B*, 2013, **183**, 81–86.
25 Y. Wang, W. Z. Jia, T. Strout, A. Schempf, H. Zhang, B. Li, J. H. Cui and Y. Lei, *Electroanalysis*, 2009, **21**, 1432–1438.
26 R. N. Bulakhe, S. V. Patil, P. R. Deshmukh, N. M. Shinde and C. D. Lokhande, *Sens. Actuators, B*, 2013, **181**, 417–423.
27 H. Steinebach, S. Kannan, L. Rieth and F. Solzbacher, *Sens. Actuators, B*, 2010, **151**, 162–168.
28 X. F. Song, L. Gao and S. Mathur, *J. Phys. Chem. C*, 2011, **115**, 21730–21735.
29 C. Y. Lee, C. M. Chiang, Y. H. Wang and R. H. Ma, *Sens. Actuators, B*, 2007, **122**, 503–510.
30 A. Aslani, V. Oroojpour and M. Fallahi, *Appl. Surf. Sci.*, 2011, **257**, 4056–4061.
31 L. Xu, R. F. Zheng, S. H. Liu, J. Song, J. S. Chen, B. Dong and H. W. Song, *Inorg. Chem.*, 2012, **51**, 7733–7740.
32 N. V. Hieu, P. T. H. Van, L. T. Nhan, N. V. Duy and N. D. Hoa, *Appl. Phys. Lett.*, 2012, **101**, 253106.
33 Z. J. Wang, Z. Y. Li, J. H. Sun, H. N. Zhang, W. Wang, W. Zheng and C. Wang, *J. Phys. Chem. C*, 2010, **114**, 6100–6105.
34 P. Lv, Z. A. Tang, J. Yu, F. T. Zhang, G. F. Zhang, Z. X. Huang and Y. Hu, *Sens. Actuators, B*, 2008, **132**, 74–80.
35 M. Bao, Y. J. Chen, J. M. Ma, F. Li, T. Lv, Y. J. Tang, L. B. Chen, Z. Xu and T. H. Wang, *Nanoscale*, 2014, DOI: 10.1039/c3nr05268k.
36 J. M. Ma, J. Teo, L. Mei, Z. Y. Zhong, Q. H. Li, T. H. Wang, X. C. Duan, J. B. Lian and W. J. Zheng, *J. Mater. Chem.*, 2012, **22**, 11694–11700.
37 B. Sun, J. Horvat, H. S. Kim, W. S. Kim, J. H. Ahn and G. X. Wang, *J. Phys. Chem. C*, 2010, **114**, 18753–18761.
38 P. Sun, Z. Zhu, P. L. Zhao, X. S. Liang, Y. F. Sun, F. M. Liu and G. Y. Lu, *CrystEngComm*, 2012, **14**, 8335–8337.
39 J. M. Ma, J. Q. Yang, L. F. Jiao, Y. H. Mao, T. H. Wang, X. C. Duan, J. B. Lian and W. J. Zheng, *CrystEngComm*, 2012, **14**, 453–459.